Deformational Styles in the Proterozoic Pinal Schist, Pinal Peak, Arizona: Microstructural and Quartz *c*Axis Analyses[1]

Myra Keep and Vicki L. Hansen
Department of Geological Sciences, Southern Methodist University, Dallas, TX 75275

ABSTRACT

A >5 km thick, north-dipping shear zone in the Pinal Peak map area, near Globe, Arizona, reveals contact metamorphism of the Pinal Schist through intrusion of the Proterozoic Madera Diorite. In Pinal Schist, sillimanite and rare andalusite occur in the metamorphic aureole around the diorite, but not elsewhere in this or adjoining map areas, where metamorphic grade is interpreted to be low greenschist facies. Deformation was synchronous in the schist and the diorite and is recorded by a well-developed, generally N- and NW-trending elongation lineation. Field interpretations of ductile deformation fabrics generally indicate top-to-the-south or reverse (present day coordinates) displacement. Microstructures in the Pinal Schist, the Madera Diorite, and the Pinal-Madera contact zone include S-C fabrics, mica "fish," asymmetric σ-type tails on porphyroclasts, and grain-shape and lattice-preferred mineral orientation, most of which indicate top-to-the-south (locally SE to SW) displacement, consistent with field interpretations. Some microstructures indicate top-to-the-north, or normal dip-slip, shear. Sillimanite is deformed into parallelism with other microstructures, indicating that it was involved in the deformation. Asymmetric double girdle quartz *c*-axis fabrics record dominantly top-to-the-south displacement, although top-to-the-north and sinistral fabrics are preserved locally. Symmetric girdles indicate deformation within the flattening ($k < 1$) field. The spatial distribution of symmetric and asymmetric girdles defines several structural domains within the shear zone. We interpret these domains to reflect large-scale strain partitioning. Equal area stereo plots of quartz *c*-axis data display clustering of maxima toward the center of the plots, suggesting activation of high-temperature slip systems. Coexistence of low-temperature deformation fabrics indicates continued deformation at progressively lower temperatures during pluton cooling. From this structural analysis we conclude that the Madera Diorite was pre-tectonic and that Pinal Schist and Madera Diorite were deformed synchronously, at relatively shallow crustal levels, in a contractional shear zone. The overall character of the shear zone reflects strain partitioning at a crustal scale.

Introduction

Southeast Arizona is one of three distinct NE-trending crustal provinces in Arizona (Bennett and DePaolo 1987; Wooden 1991; Wooden and DeWitt 1991). The Pinal Schist, metamorphosed quartz wacke turbidites, volcanic rocks, and quartzites of Proterozoic age (32°–33.5°N, 109°–112°W) (e.g., Ransome 1903; Condie and DeMalas 1985; Erickson 1968; Drewes 1981; Condie et al. 1985; Copeland and Condie 1986; Cooper and Silver 1964), represents part of a 1300 km width of juvenile crust added to the SW margin of the Archean Wyoming craton between 1800 and 1600 Ma (Van Schmus and Bickford 1981; DePaolo 1981; Stacey and Hedlund 1983; Nelson and DePaolo 1985, 1985). This crustal building event traditionally has been called the Mazatzal orogeny (Wilson 1939; Van Schmus and Bickford 1981; Condie 1982; Anderson 1986, 1989), but recent workers (e.g., Conway and Silver, 1989; Karlstrom and Bowring, 1988) suggest that the term be restricted to 1675–1625 Ma contractional deformation in southeast Arizona, to differentiate it from older, multiple tectonic events in northwest Arizona. We follow the latter convention, in which the Pinal Schist forms the extensive southeastern section of the orogen.

Although studies of the deformational and metamorphic history of the Pinal Schist are few (Swift 1987; Sease 1993; Keep and Hansen 1991, 1993), tectonic models for the Mazatzal Orogeny have the Pinal Schist as: (1) a distinct tectonic block (Karlstrom et al. 1987; Karlstrom and Bowring 1988; Bowring and Karlstrom 1990); (2) part of

[1] Manuscript received August 6, 1993; accepted November 5, 1993.

[The Journal of Geology, 1994, volume 102, p. 229–242] 0022-1376/94/10202-002$1.00

an E-trending geosyncline (Cooper and Silver 1964); (3) a large basin or series of closely related contemporaneous basins of continental margin character, possibly rift-related (Conway and Silver 1989; Condie and DeMalas 1985); (4) a continental margin-arc system and an intra-arc basin (Copeland and Condie 1986); and (5) a back arc basin (Anderson 1986, 1989). These models are difficult to differentiate structurally, but a good understanding of the style, extent, timing and crustal level of deformation within the Pinal Schist will help constrain the age, character, and extent of the deformation. This in turn will have implications for the various tectonic models, and help elucidate the character of the Mazatzal orogeny.

This study focuses on deformation styles in the Pinal Mountains, the known northern limit of the Pinal Schist. We use field and microstructural kinematic data, and quartz *c*-axis fabric analysis to determine the orientation, style, displacement sense, relative timing and crustal level of deformation in the Pinal Peak quadrangle. Few Proterozoic packages in SW North America have been scrutinized using these modern structural techniques.

Pinal Peak Quadrangle

The Pinal Peak 7 1/2 minute quadrangle, 12 miles SW of Globe, covers the central part of the Pinal Mountains (figure 1). It is underlain by a Proterozoic granitic intrusion, or series of intrusions, collectively referred to as the Madera Diorite (Ransome 1904). Well-maintained hiking trails fan out from Pinal Peak to all sides of the mountain and expose sections of both Pinal Schist and Madera Diorite. Complex interfingering of the schist and the diorite is shown schematically in figure 2.

Pinal Schist. Pinal Schist in the map area comprises a series of greenschist facies quartz-muscovite schists and interbedded quartzites preserved as roof pendants within the Madera Diorite. A well-developed metamorphic foliation parallels preserved bedding and generally dips moderately N to NW. An elongation lineation (Le), preserved along planes of foliation, plunges moderately to the N-NW (figure 2). Approximately 10 to 50 m from the diorite contact, sillimanite and rare andalusite appear in the schist, and foliation is more strongly developed than in adjacent lower-grade Pinal Schist. Sillimanite, which parallels foliation (S), occurs as long, thin ribbons, locally curved into parallelism with shear surfaces (C). Temporal relations of rare andalusite with respect to deformation are difficult to discern uniquely due to the small grain size and equant habitat of the crystals. A "hybrid" unit, lacking foliation and comprising elements of both schist and diorite, marks the contact. Foliation and Le are similarly oriented within the high-grade and low-grade schist.

Madera Diorite. "Madera Diorite," first proposed by Ransome (1903) to describe Proterozoic intrusions throughout the Pinal Schist in the Pinal Mountains, comprises andesine-quartz-biotite intrusives with minor orthoclase or microcline and accessory hornblende, magnetite, apatite, and zircon (Ransome 1903). Rb-Sr data provide an absolute age of 1690 Ma (uncorrected) for the Madera Diorite (Livingston, 1969). In the Pinal Peak quadrangle Ransome (1903) recognized massive to strongly foliated phases; three types of granitoid occur. Around Madera Peak in the NW part of the quadrangle, diorite is fine-grained, of intermediate composition, with a color index of 30. Quartz occurs as 3 mm to 1 cm large anhedral grains, plagioclase feldspar as millimeter size grains, and the mafic mineral is predominantly finely crystalline biotite. The southern slopes of Pinal Peak expose a coarser granitic rock with a similar mineralogy and a color index of 15. On the north side of the peak, a coarse granitic rock (color index 15–20) with centimeter scale phenocrysts crops out. Lack of exposed contacts results in poor understanding of the spatial and genetic relationships between these intrusive rocks. We follow the suggestion of Ransome (1919) and Wilson et al. (1969) that these granites comprise a single intrusive unit. A U-Pb zircon age is in progress.

Shear Zones. High-angle, E- to NE-striking, anastomosing ductile shear zones, varying in width from tens of centimeters to tens of meters, cut both the Madera Diorite and the Pinal Schist (figure 3). Within these zones individual small-scale shear zones, developed on a scale of centimeters to meters, vary in width and separate regions of massive, relatively undeformed rock (figure 3). Moderately to well-developed S-C fabrics (Berthé et al. 1979; Lister and Snoke 1984) characterize the deformation. These fabrics result from strain partitioning and comprise a schistosity (S) at an angle to the shear zone boundary, cut by a second set of shear planes (C) parallel to the boundary. The S-C fabrics preserved in these zones of high strain allow interpretation of the sense of movement of the shear zone (Berthé et al. 1979; Simpson and Schmid 1983; Lister and Snoke 1984; Passchier and Simpson 1986; Simpson 1986) (figure 2).

Figure 3*a* represents schematically the nature of the shear zones in the Pinal Peak quadrangle. Anastomosing shear zones dip moderately north, parallel or sub-parallel to metamorphic foliation. They

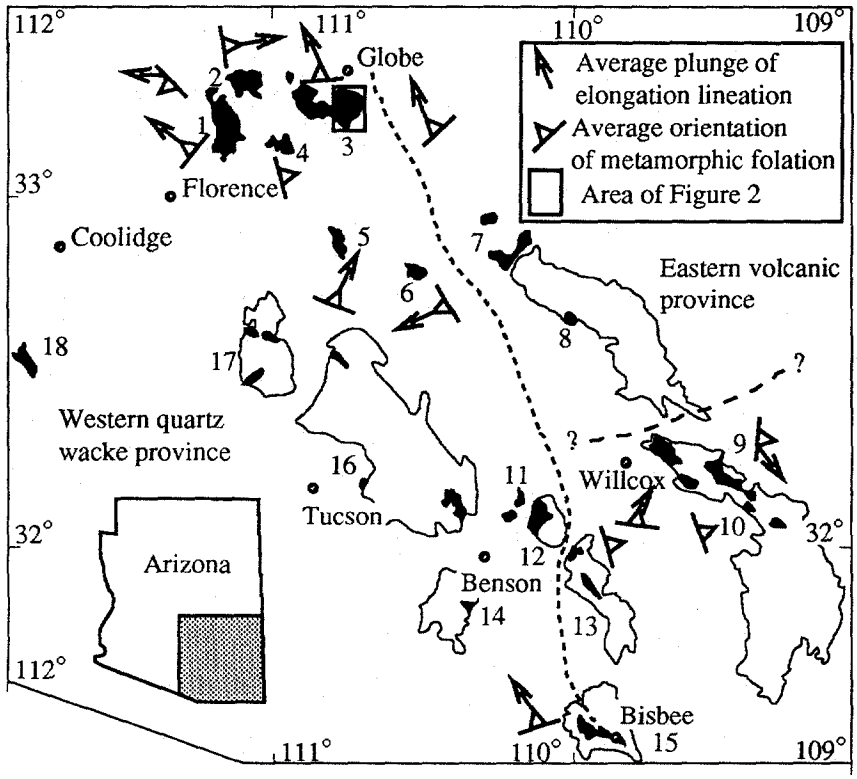

Figure 1. Outcrops of Pinal Schist in SE Arizona (black), and nearby towns. Outlined areas are larger mountain belts where Pinal Schist crops out: 1 = Mineral Mountain; 2 = Superior area; 3 = Pinal Mountains; 4 = Teapot Mountain; 5 = Winkelman area; 6 = Holy Joe Peak; 7 = Santa Teresa Mountains; 8 = Pinaleño Mountains; 9 = Dos Cabezas Mountains; 10 = Chiricahua Mountains; 11 = Johnny Lyon Hills; 12 = Little Dragoon Mountains; 13 = Dragoon Mountains; 14 = Whetstone Mountains; 15 = Mule Mountains; 16 = Santa Rita Mountains; 17 = Santa Catalina Mountains; 18 = Slate Mountains. Short-dashed line is the province boundary of Copeland and Condie (1986); large-dashed line is the proposed boundary of Anderson (1986, 1989) separating the Dos Cabezas rhyolite province from the Pinal Schist. Symbols represent average orientation of metamorphic foliation and elongation lineation for Pinal Schist in SE Arizona. Data for northern Dos Cabezas Mountains from Sease and Hansen (1990) and Sease (1993); for Mineral Mountain from Theodore et al. (1978) and Keep and Hansen (1991); remaining data from Keep and Hansen (1993) and Keep (unpublished).

occur either entirely within the Pinal Schist or Madera Diorite, or may encompass both units. Material possessing no strong foliation, Le, or S-C structures occurs between the shear zones. These largely undeformed zones have sharp, centimeter scale boundaries with the sheared material. Figure 3*b* illustrates components of an individual shear zone within the Pinal Schist. Characteristic mesostructural fabrics include moderately to well-developed S and C planes and generally well-developed Le. Field interpretations of displacement within these shear zones are assigned a confidence level from 1 (low) to 5 (high) depending on the degree of development (related to the amount of strain and host lithology) of the S-C fabrics. Deformed samples of Pinal Schist, where interpretable, record a consistent top-to-the-south, or reverse, sense of shear (present day coordinates) (figure 2), with confidence levels of 4 and 5. Massive zones between highly sheared areas in the Pinal Schist preserve bedding and areas of chaotic folds characterized by inconsistent folding styles, marked changes in bed thickness, and varying fold axis orientation. Shear zone boundaries cross-cut these folded areas, indicating that folding pre-dates shear zone deformation. We interpret these regions of chaotic structures as soft sediment slumps. Locally less deformed regions within the Pinal Schist are not folded; they are characterized by uniformly foliated schist with bedding-parallel foliation and general northerly dip. Sharp boundaries (cm scale) separate deformed and less-deformed material.

Figure 3*c* illustrates a shear zone within Madera Diorite. Within shear zones that cut the diorite,

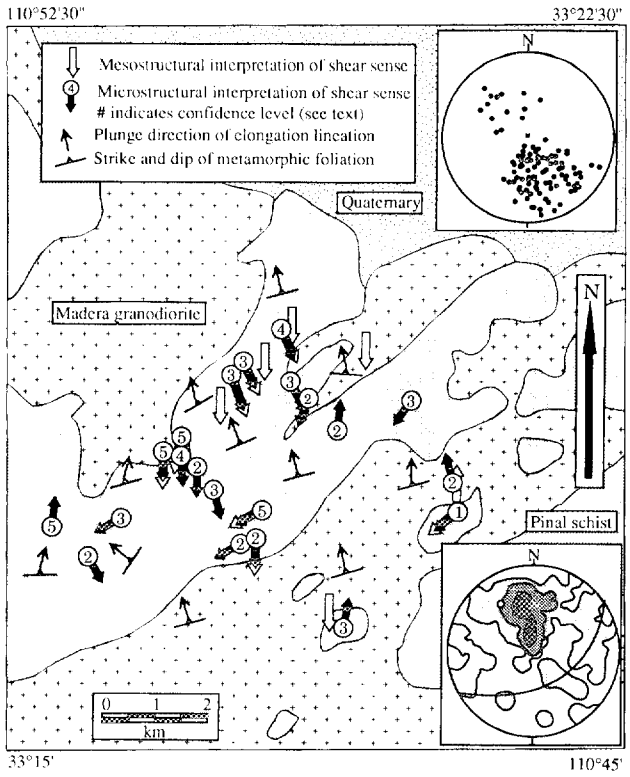

Figure 2. Geologic map of the Pinal Peak map area showing field and microstructural kinematic data. Lower hemisphere stereonet at top right shows poles to metamorphic foliation; plot at bottom right shows contoured elongation lineation with contours at 0.7, 3, 5.4, 7.8, 10.1 and 12.5. Great circle represents poles to average foliation plane, with pole shown as open circle.

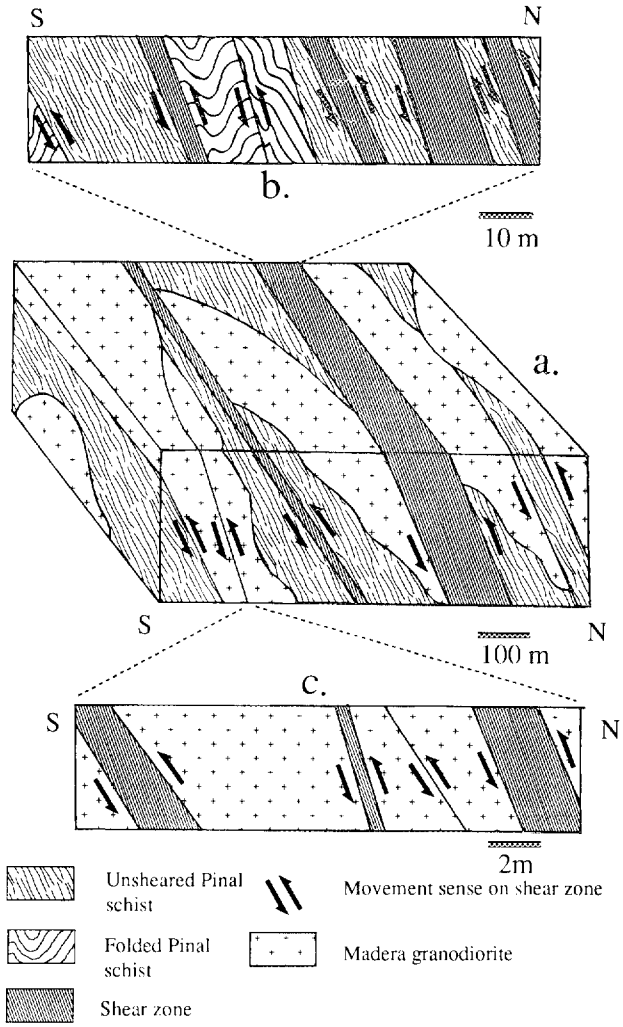

Figure 3. (*a*) Schematic block diagram illustrating spatial relationships between the Pinal Schist, Madera Diorite and shear zones. See text for discussion. (*b*) Detail of an individual shear zone within the Pinal Schist. (*c*) Detail of an individual shear zone within the Madera Diorite.

S-C fabrics and quartz porphyroclasts with σ-type asymmetric tails (Berthé et al. 1979; Simpson and Schmid 1983) record top-to-the-south (reverse) shear sense during ductile deformation (figure 2). These zones of ductile deformation have sharp boundaries (centimeter scale) with zones of massive, undeformed diorite.

The relatively consistent orientation of metamorphic foliation and Le throughout the Pinal Peak quadrangle (figure 2) indicates a minimum structural thickness of 5.4 km for Pinal Schist within the quadrangle (based on an average dip of 58°). Variations in strike along the transect define the anastomosing style.

Microstructures. Microstructural examination of selected samples of Pinal Schist and Madera Diorite involved motion plane sections (perpendicular to foliation, containing Le). Common microstructures include S-C fabrics, microfolding, grain-shape preferred orientation of quartz and muscovite, lattice preferred orientation of quartz, mica "fish," sigma-shaped quartz grains, monocrystalline quartz ribbons, and fractured quartz grains (Berthé et al. 1979; Simpson and Schmid 1983; Passchier and Simpson 1986; Simpson 1986) (figure 4). Of these microstructures, monocrystalline quartz ribbons and fractured quartz grains are typical of, and the others consistent with, low-temperature deformation (Bouillier and Bouchez 1978; Simpson 1985). Sillimanite, where observed, displays "fish" and elongate, sigma-shaped grains similar in orientation to adjacent quartz and muscovite microstructures (figure 4), inferring that sillimanite pre-dated and was involved in the shear zone deformation. Rare andalusite has no preferred orientation, and the small, equant character of the grains does not allow a unique interpretation of its age relative to deformation.

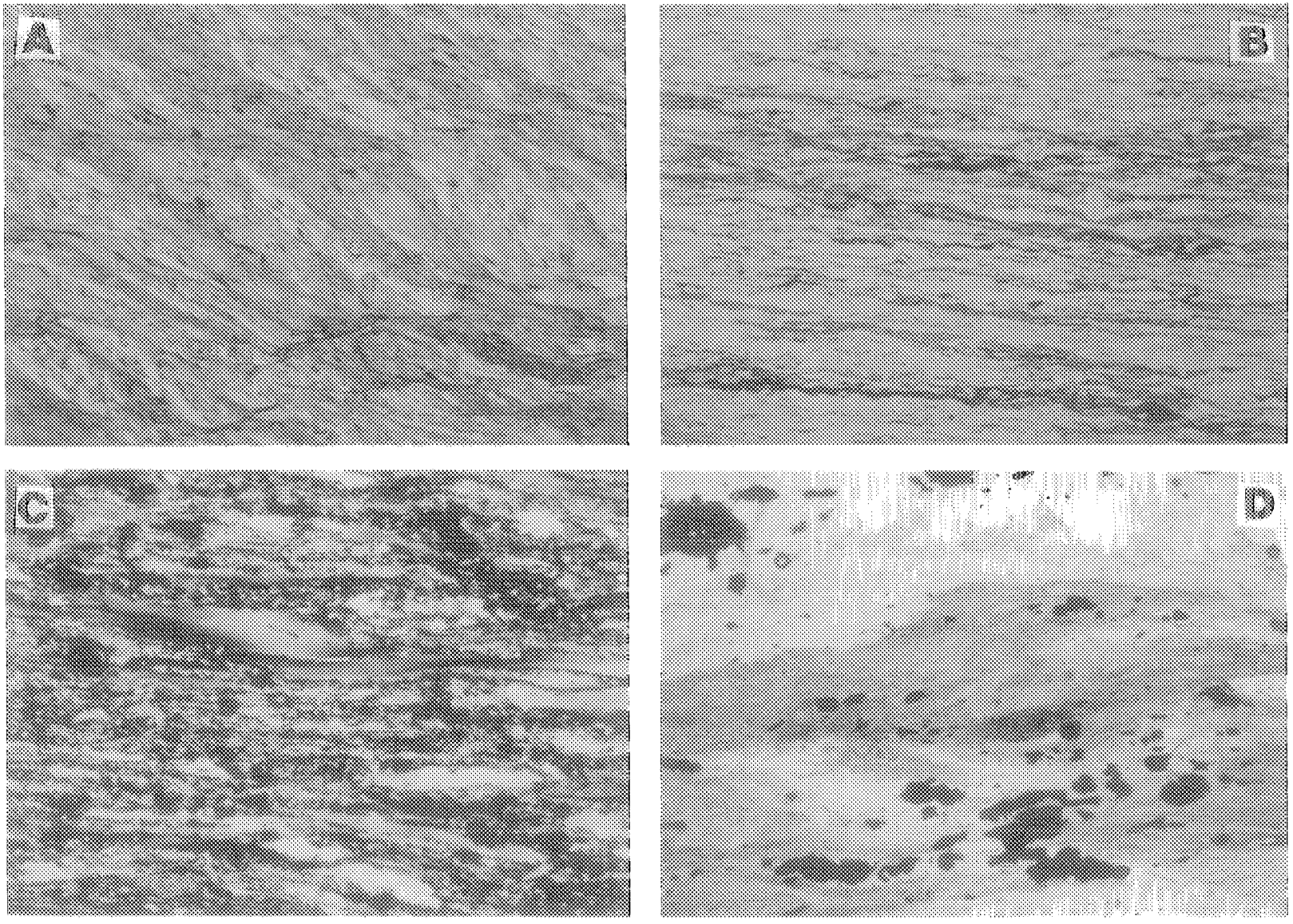

Figure 4. Photomicrographs showing examples of microstructures described in the text. All plates are 9 mm wide. (*a*) S-C fabric in Pinal Schist, sample P195, viewed to the northwest. Fabrics indicate top-to-the-southwest motion. (*b*) S-C fabrics, strained quartz and σ-type quartz porphyroclasts with tails in Pinal Schist, sample P189. Photomicrograph is viewed to the northeast. Fabric indicates top-to-the-southeast motion. (*c*) Strained quartz in Pinal Schist, sample P200, viewed to the northeast. *c*-axes from all three samples are shown in figures 6 and 7. (*d*) Sigmoidal sillimanite grains, sample P203, viewed to the southeast. Fabric indicates top-to-the-southwest motion. P195 falls in the domain of non-coaxial shear; P189 and P200 fall in the variable flattening domain. *c*-axes were not measured for P203.

Microstructures record predominantly reverse (top-to-the-south or S-SE, present day coordinates) displacement (figure 2); interpretations are assigned a confidence level of 1 (low) to 5 (high). Four samples record top-to-the-north displacement. These samples include both Pinal Schist and Madera Diorite, are broadly distributed in the field area (figure 2), and have confidence levels varying from 2 to 5 on the basis of S-C fabrics, biotite and muscovite "fish," grain-shape preferred orientation of biotite, muscovite and quartz, and folding of graphite bands. These samples may record normal dip-slip motion. In addition, four samples record top-to-the-southwest displacement. These samples include both Pinal Schist and Madera Diorite and are distributed in a narrow, E-W band in the southern part of the map area. Movement sense is interpreted on the basis of long, stretched out sillimanite grains, well-developed S-C fabrics, sigmoidal quartz grains, mica "fish," epidote porphyroclast tails, grain-shape preferred orientation of quartz and fractured plagioclase grains: confidence levels vary from 1 to 5. These samples represent a narrow band of strike- or oblique-slip displacement within the overall reverse shear zone.

Quartz c-axis Analysis. *c*-axis fabrics of quartz may help to determine shear sense in plastically deformed rocks (e.g., Sander 1970; Lister 1977; Lister and Williams 1979; Lister and Hobbs 1980; Behrmann and Platt 1982; Passchier 1983; Bouchez et al. 1983; Schmid and Casey 1986; Law 1990). Sections chosen for fabric analysis have well-developed lattice-preferred orientation of quartz. Measurements were taken in the motion plane, which contains the XZ finite strain axes, and in the plane containing the YZ plane finite strain axes (perpendicular to both foliation and Le) (Carreras et al. 1977), with a minimum of 250 measurements per plane (500 per sample) (Miller and Christie 1981). YZ plane measurements are rotated into parallelism with those of the motion plane. Resulting girdle patterns are perpendicular to Le and may be symmetric or asymmetric. Such fabrics are indicative of ductile deformation (e.g., Lister and Hobbs 1980), supporting the interpretation that measured lineations are elongation lineations (related to the direction of tectonic transport) (e.g., Law et al. 1994) and not intersection lineations. Girdle patterns reflect total strain (e.g., Lister and Williams 1979). Older fabrics may be partially reset by additional plastic deformation (Lister and Price 1978), although experimental studies (Ralser et al. 1991) suggest that even up to large strains (60%), evidence of older fabrics may survive. Symmetric fabrics may result from simple coaxial flattening, or from partial overprinting of opposite asymmetries, giving total apparent pure shear. The sense of asymmetry of a fabric, and its obliquity to the foliation (i.e., the angle between the foliation normal and the intersection of the girdle axis with the XZ plane), indicate the sense of shear (Lister and Hobbs 1980; Behrmann and Platt 1982; Schmid and Casey 1986; Lister 1977; Starkey 1987; Law 1990).

Figure 5 illustrates *c*-axis data and interpreted movement sense, including both symmetric and asymmetric double girdle fabrics, from three samples of Madera Diorite and 10 samples of Pinal Schist. Lower hemisphere equal area plots of *c*-axis data are viewed to the west, except for samples P195 and P196B, which are viewed to the northwest. Samples P167, M183, M184A, P184B, P185, and P195 shows strong symmetric double girdle fabrics (Sander 1970; Lister 1977) indicative of noncoaxial shear (Schmid and Casey 1986). These fabrics record top-to-the-north (M183, M184A), top-to-the-south (P167, P184B, P185), and left-reverse motion (P195) in map view (figure 6). The *c*-axis fabric for sample P196B has elements of both oblique-slip shear and coaxial flattening (see below). Top-to-the-north and oblique-slip displacements contradict the top-to-the-south movement sense recorded by the majority of field and thin section interpretations (figure 2), but provide independent corroboration of local normal and oblique-slip motion postulated from microstructural observations. Both samples with top-to-the-north *c*-axes have top-to-the-south grain-shape preferred orientation of quartz. Symmetric girdles, indicative of ductile deformation but not of shear sense, are recorded by samples P189, P192, P194B, P200, G229, and P232. Of this group, samples P194B, P200, G229, P232, and possibly P196B have fabrics predicted for deformation in the flattening field ($k < 1$), characterized by small circle distributions of *c*-axes centered around the pole to foliation (Price 1985; Schmid and Casey 1986; Law 1990). The same samples also contain microstructures that yield interpretable movement directions (i.e., noncoaxial shear). The *c*-axis fabrics therefore represent a component of flattening and a component of non-coaxial shear, resulting in overall bulk flattening. Figure 6 shows *c*-axes plots and interpreted shear directions in map view. An approximately vertical line extending from the right of P189 to the left of P194B separates a western domain of asymmetric girdles (non-coaxial shear) from an eastern domain of symmetric girdles (bulk flattening). P196B is located on the domain boundary.

Clustering of maxima toward the center of *c*-

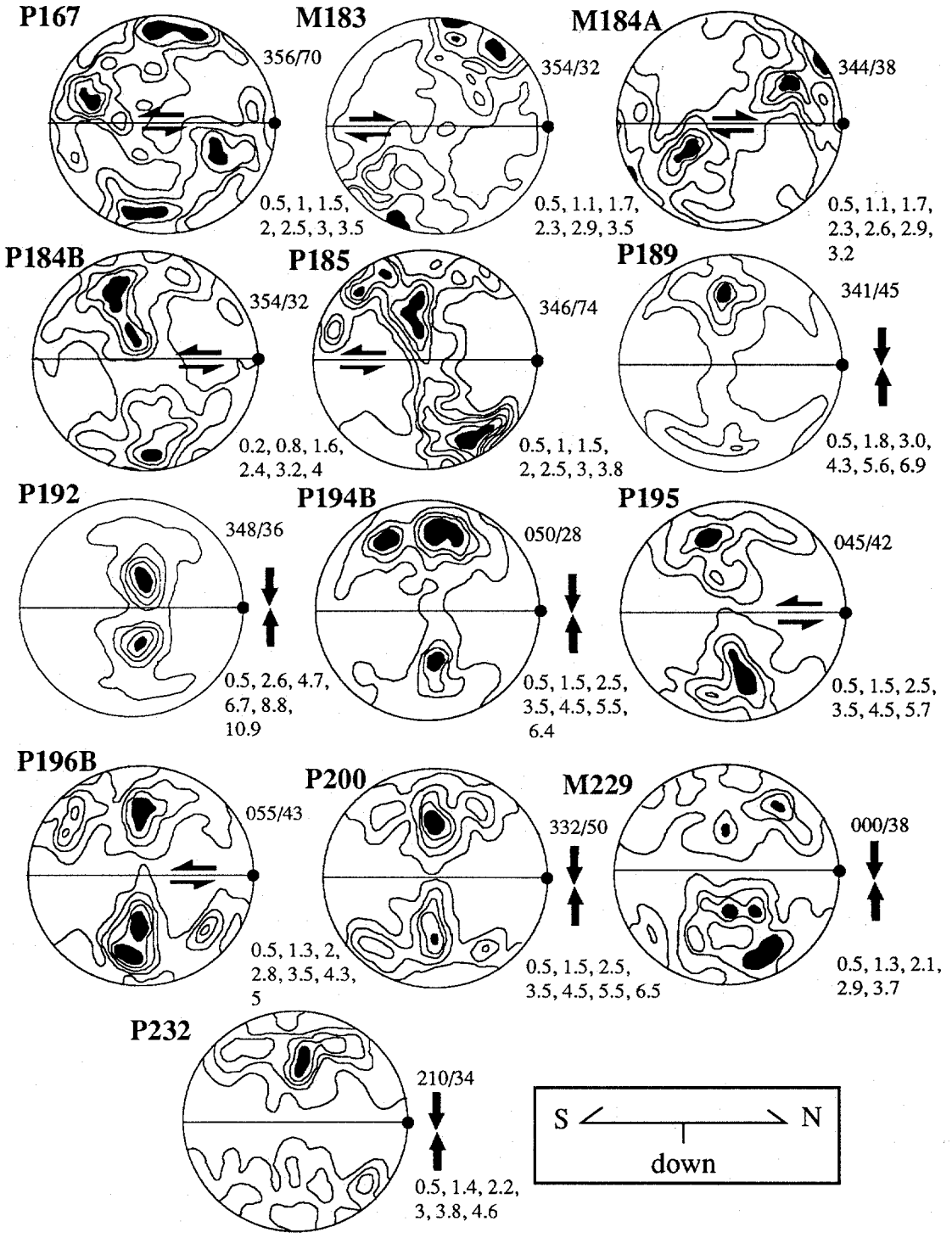

Figure 5. Contoured equal area, lower hemisphere stereographic projections of quartz *c*-axis data. Sample numbers are shown to the top left of plot, with contour intervals shown at bottom right. Numbers at top right are trend and plunge of elongation lineation, represented by black dots on right hand side of each plot. Vertical east-west plane represents metamorphic foliation (S). $N = 500$ points for each plot. Viewing direction is to the west except for samples P195 and P196B, which are viewed to the northwest.

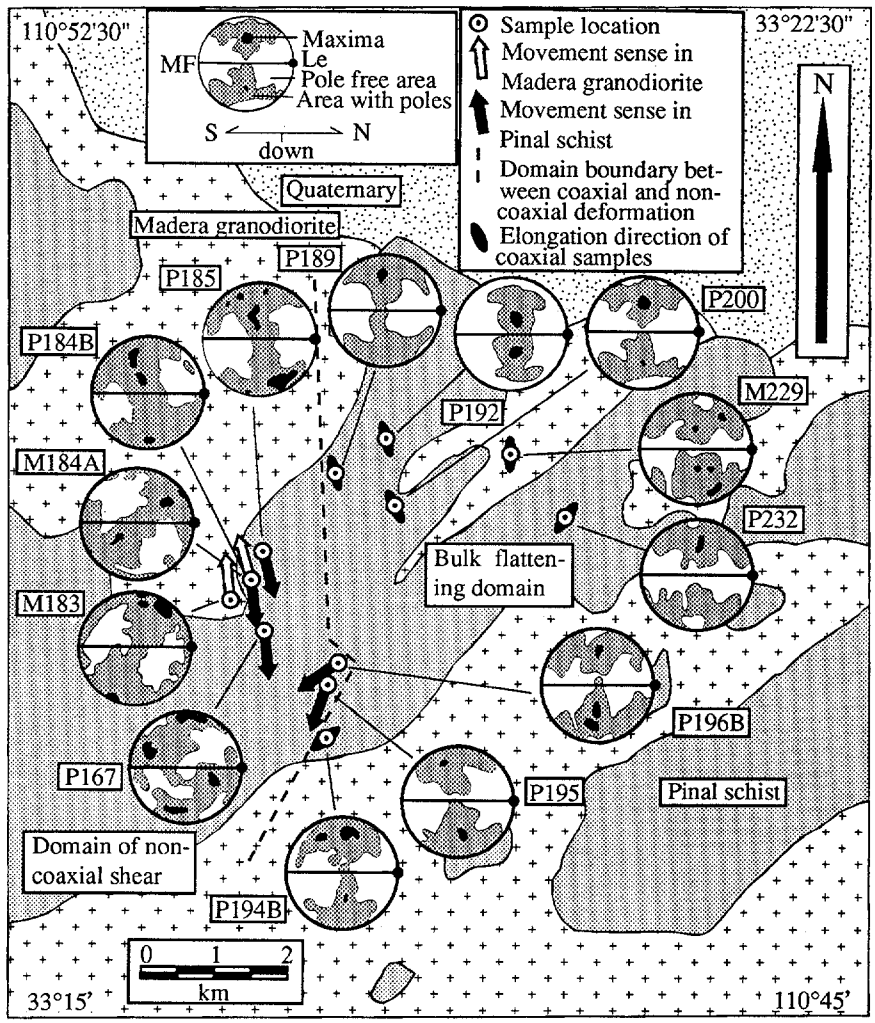

Figure 6. Geologic map of the Pinal Peak map area showing the locations and contoured plots (see figure 5) of quartz *c*-axis fabrics. Where no arrows are shown, fabric is symmetric recording bulk coaxial strain; elongation direction of these samples is shown by the black ellipses. Viewing direction for stereonet plots is to the west except for samples P195 and P196B, which are viewed to the northwest.

axis stereonet plots illustrates activation of progressively higher temperature slip systems in quartz (Jessell and Lister 1990) and the possibility of interaction of two or more regimes of dislocation creep (Hirth and Tullis 1992). Basal ⟨a⟩ slip occurs at low temperatures and high strain rates, with increasing temperatures causing rhombohedral ⟨a⟩ and ultimately prismatic ⟨a⟩ slip systems to operate (Tullis et al. 1973; Tullis 1977; Lister and Dornsiepen 1982). Stereonet plots from the domain of non-coaxial shear display both basal and rhombohedral ⟨a⟩ slip characteristics; those from the bulk flattening domain display only rhombohedral ⟨a⟩ characteristics. In addition, P167 and G184A display maxima that may represent prism ⟨c⟩ slip, a system not commonly recorded (Garbutt and Teyssier 1991). Prism ⟨c⟩ slip is most commonly associated with high-temperature deformation (e.g., Garbutt and Teyssier 1991) and intense hydrolytic weakening of quartz (Behr 1980; Blumenfeld et al. 1986; Dubendorfer and Houston 1987). Samples with potential prism ⟨c⟩ maxima are all within the domain of non-coaxial shear, and their significance is not fully understood. Activation of high-temperature rhombohedral ⟨a⟩ slip systems in Pinal Schist and Madera Diorite suggest deformation began soon after emplacement of the diorite. However, the relative abundance of low-temperature microstructures (e.g., monocrystalline quartz ribbons and fractured quartz grains), and the presence of deformed sillimanite suggest that either deformation continued during cooling (with high-temperature fabrics surviving progressively lower-temperature strain), or that high-temperature deformation is spatially limited to pluton margins, with low-temperature deformation occurring away from the intrusion. Complex interfingering of Pinal Schist and Madera Diorite, and poor exposure away from hiking trails, prevents testing the hypothesis of a spatial relationship between high-temperature slip and proximity to the Madera intrusions. We propose that deformation

commenced soon after pluton intrusion, and continued at progressively lower temperatures as the pluton cooled.

Discussion

Approximately 5 km of a N-dipping, dominantly reverse, shear zone is exposed in the northern Pinal Mountains. Rocks cut by the shear zones display S-C fabrics developed contemporaneously in the schist and the diorite. The S-C fabrics and microstructures indicate a general top-to-the-south (locally top-to-the-southeast), or reverse sense of shear within individual samples, in present day coordinates, with local top-to-the-north and left-reverse-slip. Quartz *c*-axis fabric data indicate top-to-the-north, top-to-the-south and strike-slip displacement. Local strike-slip displacement (P195, P196B) occurs in the southern part of the map-area: top-to-the-north and top-to-the-south displacement both occur in the central and northern areas (figure 6).

Potential Reasons for Conflicting Movement Senses within Samples. Microstructures in M183 and M184A record top-to-the-south displacement. Quartz grain-shape preferred orientation also reflects top-to-the-south displacement, although quartz *c*-axis fabrics from the same samples indicate top-to-the-north motion. The conflicting quartz *c*-axis fabrics may reflect the polymineralic nature of both samples (Madera Diorite), which has been shown to disperse developing crystallographic fabrics and reduce the quality of quartz *c*-axis data (Starkey and Cutforth 1978; Schmid and Casey 1986). However, the *c*-axis fabrics show definite asymmetric girdles. Quartz *c*-axis girdles locally inclined in a direction opposite to the overall sense of shear have been reported from West Germany and the Eastern Alps (Krohe 1990), and from quartz ribbons in the Cap de Creus mylonites of NE Spain (Carreras et al. 1977; Garcia Celma 1982). In both areas the authors interpreted the aberrant quartz *c*-axis to be non-representative of shear direction, and argued for caution in interpreting quartz *c*-axis data. Hansen (1990, unpublished) finds that in the Tally Ho shear zone of the Canadian Cordillera, quartz grain-shape preferred orientation records early amphibolite-grade sinistral shear, whereas quartz *c*-axis fabrics within the same sample record an interpreted younger, greenschist-grade dextral event. Law et al. (1994) similarly describe skeletal quartz *c*-axis fabrics that record an opposite shear sense to that interpreted from both the observed sense of obliquity between foliation and grain alignment of quartz and the complete (i.e., non-skeletal quartz *c*-axis fabric. In pure quartzites, *c*-axes recording opposite movement directions are used as evidence for potential unreliability of quartz *c*-axis analysis (Passchier 1983).

We do not fully understand the reasons for aberrant *c*-axis fabrics. Such fabrics may simply indicate that *c*-axis fabric interpretations are not entirely reliable (e.g., Carreras et al. 1977; Garcia Celma 1982; Passchier 1983; Krohe 1990; Law 1990). Alternately, if, as suggested by Ralser et al. (1991), *c*-axis fabrics retain their integrity through large additional strains (up to 60%), then the aberrant fabrics may be recording an earlier phase of deformation. This effect may be enhanced if older fabrics formed at higher temperatures than younger fabrics. A third possibility is that reorientation of quartz *c*-axes with respect to the host grain may take place during mild, late-phase deformation, during which quartz *c*-axes may be preferentially reoriented with respect to the rock fabric. In this case the top-to-the-north movement recorded in the *c*-axes would represent late normal slip on the shear zone. Such a mechanism requires *c*-axis girdle patterns to record preferentially the last episode of strain (Lister and Price 1978), a conclusion countered by the experimental work of Ralser et al. (1991). Both Pinal Peak samples with aberrant *c*-axes girdles are Madera Diorite: both have definite asymmetric *c*-axis fabrics and cannot simply be disregarded because they do not fit the general pattern. We propose that *c*-axis fabric development in these granitoids (M183 and M184A) is related to temperatures during microstructural formation, by mechanisms which we do not fully understand.

Spatial Distribution of Structural Domains. Within the Pinal Peak quadrangle, kinematic indicators record top-to-the-south, top-to-the-north and left-reverse displacement. In addition, quartz *c*-axis fabrics define two structural domains, one of non-coaxial shear and one of bulk flattening ($k < 1$) (figure 6). The simplest boundary between the variable flattening and non-coaxial domains is approximately perpendicular to strike (figure 6), indicating along-strike changes in deformation history over approximately 6 km. Along-strike changes in deformation history are difficult to explain. One hypothesis is that the domain boundary is controlled by the underlying contact between Pinal Schist and Madera Diorite. Fabrics from samples centered over the main body of the pluton may have been affected by increased temperature, possibly resulting in increased grain recrystallization and overprinting of original asymmetric fabrics. However, contacts between Pinal Schist and Madera Diorite

are complexly interfingered, and the variable flattening domain does not correspond with even the generalized contacts between Pinal Schist and Madera Diorite (figure 6). An alternate hypothesis is that there are several domain boundaries, oriented generally parallel to strike (figure 7*a*). In this model, the exposed structural section of the shear zone is viewed as a large-scale ductile deformation fabric, with strain partitioning resulting in juxtaposition of zones of differing strain intensity (Lister and Williams 1983; Gapais et al. 1987). Although the mechanism for strain partitioning is unknown, it is possible that some bands within the Pinal Schist are preferentially flattening in response to deformation, while others deform by non-coaxial shear (both dip- and strike-slip). The overall effect, illustrated in figure 7, would be similar to squeezing and shearing an Oreo cookie at room temperature: the cream filling would bulge out (flattening > shear) with the chocolate layers sliding over the top.

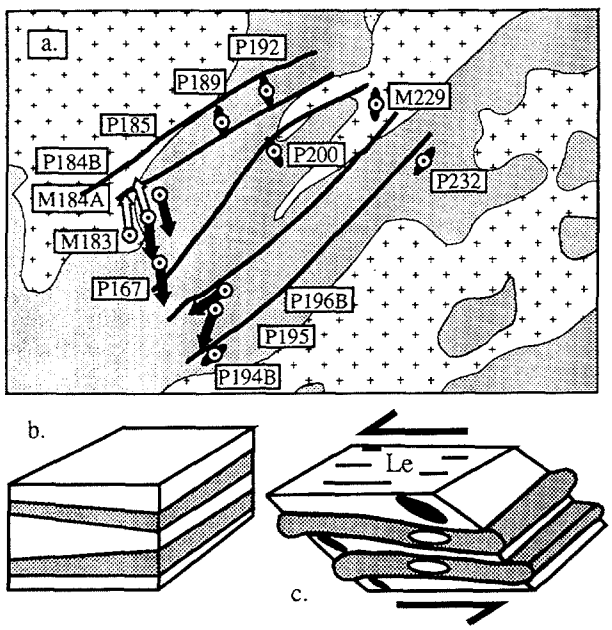

Figure 7. Alternate model for strain partitioning into discrete structural domains in the Pinal Peak quadrangle. (*a*) Enlargement of central part of figure 6 showing sample locations and possible location of boundaries between quartz *c*-axis domains. All symbols as in figure 6. (*b*) Schematic block diagram of Oreo cookie layering model before deformation. White layers deform by shearing, dark layers by bulk flattening. (*c*) Schematic block diagram of Oreo cookie layering model after deformation. White strain ellipses represent coaxial flattening strain in dark layers; black strain ellipses represent non-coaxial shear in white layers. Arrows show direction of shear.

We prefer this second hypothesis of several domain boundaries oriented parallel to strike (figure 7*a*) to explain the distribution of apparent coaxial and non-coaxial deformation domains in the Pinal Peak quadrangle. Strain partitioning is seen at many scales: S-C fabrics, observed in thin-section and hand sample, record evidence of strain partitioning, which is reflected by the anastomosing nature of individual shear zones and sharp boundaries between sheared and massive material in both Pinal Schist and Madera Diorite. It is therefore not surprising that the overall character of the shear zone incorporates similar partitioning components. In addition, this model easily allows for zones of strike/oblique-slip (if your thumb slips on the cookie), reflected in the central part of the map area.

Possibility of Post-Proterozoic Rotation. The Globe area has a complex structural history (Ransome 1903; Peterson 1962; Cornwall and Krieger 1978). Episodes of widespread faulting producing steeply dipping NE- and NW-striking faults are constrained to be post-Carboniferous (Mesozoic?), Mesozoic-Tertiary, and post-Tertiary in age (Peterson 1962). Faulting did not affect the crystalline massif of Madera Diorite with its roof pendants of Pinal Schist (Ransome 1903; Peterson 1962), which acted as a fault-bounded block (Peterson 1962; Cornwall and Krieger 1978). Internally, this massif has consistent orientations of metamorphic foliation (N to NW dip) and Le (N to NW plunge) over a large area, and no NE- or NW-striking faults cut the Pinal Schist or Madera Diorite. Reorientation of present day coordinates to account for block rotation may change the dominant shear sense documented in the shear zone. Although possibilities for reorientation are many, there is no geological evidence for any major rotations, and only one minor episode of block rotation is suggested. Peterson (1962) proposed that the Pinal/Madera block rotated about a NW-trending axis resulting in NE uplift and SW tilting. Reorientation to Proterozoic coordinates (i.e., SW uplift and NE-directed tilting) gives variable results depending on the degree of rotation. At small angles, the zone remains contractional, with an increasing dextral component at larger rotation angles. Given the lack of geologic evidence for large block rotations in the area, we conclude that the shear zone probably records overall crustal contraction, and that any rotations resulting from block adjustments were small.

The Significance of Contemporaneous Deformation. Deformation in the Pinal Schist and Madera Diorite is contemporaneous. Deformation styles in these units are identical, and the same shear zones

cut both of the rock types. Shear zone orientation is consistent throughout the units, with small changes in strike recording an anastomosing nature. Ductile deformation fabrics are seen in both units. The Madera Diorite is at least syn-tectonic, and the presence of deformed sillimanite indicates that peak metamorphism pre-dated deformation (i.e., the pluton is pre-tectonic). This is an important observation as Mazatzal-age granites throughout SE Arizona are key to timing the duration of the Mazatzal orogeny. Such granites have been regarded as both syn- and post-deformational (Cooper and Silver 1964), with pre-deformational granites as young as ~1660 Ma, and post-deformational plutons as old as ~1630 Ma (Conway, pers. comm.). Available Rb-Sr data provide an absolute age of 1690 Ma (uncorrected) for the Madera Diorite (Livingston 1969). U-Pb zircon analyses are in progress, and preliminary results indicate the possibility of inheritance in the Madera Diorite (Gonzales, 1993, pers. comm.). A definitive age on the Madera Diorite will help to constrain the timing of deformation of the Mazatzal orogeny in this area. No other plutons of this general age are reported in SE Arizona.

The Pinal Schist throughout SE Arizona has experienced low greenschist grade metamorphism, indicating metamorphism at relatively shallow crustal levels. High-grade metamorphism is seen around the Madera pluton, indicating that the Madera Diorite intruded at intermediate to shallow crustal levels. Similar pluton-controlled metamorphism is seen throughout SE Arizona (Williams 1991). Sillimanite and rare andalusite are not observed in contact with each other: there is also no evidence of replacement of andalusite by sillimanite, suggesting that sillimanite and andalusite may have formed synchronously. In this case, metamorphic conditions are limited to approximately 2–4 kb, 250°–450°C (Williams 1991). Activation of high-temperature slip systems in quartz indicate that deformation began during or soon after intrusion and metamorphism. However, widespread evidence of low-temperature deformation fabrics throughout the area suggests that deformation continued at progressively lower temperatures as the pluton cooled. Quartz *c*-axis plots may be showing preservation of earlier, higher temperature deformation.

Conclusions

We draw the following conclusions from this study: (1) Top-to-the-south (present day coordinates) contractional deformation affected both the Pinal Schist and Madera Diorite in the Pinal Mountains; (2) The shear zone character is that of a large-scale ductile deformation, juxtaposing domains with differing strain histories as a result of crustal-scale strain partitioning. Strain partitioning is seen at several scales within the shear zone; (3) Peak metamorphic conditions were attained prior to deformation, with sillimanite involved in the deformation; (4) Deformation was initiated at relatively high temperatures, as evidenced by the activation of high-temperature slip systems in quartz, and continued at progressively lower temperatures during pluton cooling; (5) Regional greenschist facies metamorphism indicates that the Madera Diorite intruded at relatively shallow crustal levels, with higher-grade material spatially limited to pluton margins.

ACKNOWLEDGMENTS

This work has been supported by Geological Society of America Research Grants 4481-90 and 4729-91, Sigma Xi Grants-in-Aid-of-Research, the Institute for the Study of Earth and Man at Southern Methodist University, and the Dedman College Graduate Assembly at Southern Methodist University. Our thanks to Rick Law, Laurel Goodwin and Clay Conway for their thorough and thoughtful reviews that helped clarify our thinking and improved the quality of the paper.

REFERENCES CITED

Anderson, P., 1986, Summary of the Proterozoic plate tectonic evolution of Arizona from 1900 to 1600 Ma: Arizona Geol. Soc. Digest, v. 16, p. 5–11.

———, 1989, Proterozoic plate tectonic evolution of Arizona, *in* Jenney, J. P., and Reynolds, S. J., eds., Geologic evolution of Arizona: Arizona Geol. Soc. Digest, v. 17, p. 17–55.

Behr, H. J., 1980, Polyphase shear zones in the granulite belts along the margins of the Bohemian Massif: Jour. Struct. Geol. v. 2, p. 249–254.

Behrmann, J. H., and Platt, J. P., 1982, Sense of nappe emplacement from quartz *c*-axis fabrics; an example from the Betic Cordilleras (Spain): Earth Planet. Sci. Lett., v. 59, p. 208–215.

Bennett, V. C., and DePaolo, D. J., 1987, Proterozoic crustal history of the western United States as deter-

mined by neodymium isotopic mapping: Geol. Soc. America Bull., v. 99, p. 674–685.

Berthé, D.; Choukroune, P.; and Jegouzo, P., 1979, Orthogneiss, mylonite, and non-coaxial deformation of granites: the example of the South American shear zone: Jour. Struct. Geol., v. 1, p. 31–42.

Blumenfeld, P.; Mainprice, D.; and Bouchez, J. L., 1986, *C*-slip in quartz from subsolidus deformed granite: Tectonophysics, v. 127, p. 97–115.

Boullier, A.-M., and Bouchez, J.-L., 1978, Le quartz en rubans dans les mylonites: Bull. Soc. Géol. France, v. 7, p. 253–262.

Bouchez, J. L.; Lister, G. S.; and Nicolas, A., 1983, Fabric asymmetry and shear sense in movement zones: Geol. Rundschau, v. 72, p. 401–419.

Bowring, S. A., and Karlstrom, K. E., 1990, Growth, stabilization, and reactivation of Proterozoic lithosphere in the southwestern United States: Geology, v. 18, p. 1203–1206.

Carreras, J.; Estrada, A.; and White, S., 1977, The effects of folding on the *c*-axis fabric of a quartz mylonite: Tectonophysics, v. 39, p. 3–24.

Condie, K. C., 1982, Plate tectonics model for Proterozoic continental accretion in the southwestern United States: Geology, v. 10, p. 37–42.

———, and DeMalas, J. P., 1985, The Pinal Schist: an early Proterozoic quartz wacke association in southeastern Arizona: Precamb. Res., v. 27, p. 337–356.

———; Bowling, G. P.; and Vance, R. K., 1985, Geochemistry and origin of early Proterozoic supracrustal rocks, Dos Cabezas Mountains, southeastern Arizona: Geol. Soc. America Bull., v. 96, p. 655–662.

Conway, C. M., and Silver, L. T., 1989, Early Proterozoic rocks (1710–1615 Ma) in central to southeastern Arizona, *in* Jenney, J. P., and Reynolds, S. J., eds., Geologic Evolution of Arizona: Arizona Geol. Soc. Digest, v. 17, p. 165–186.

Cooper, J. R., and Silver, L. T., 1964, Geology and ore deposits of the Dragoon Quadrangle, Cochise County, Arizona: U.S. Geol. Survey Prof. Paper 416, 196 p.

Copeland, P., and Condie, K. C., 1986, Geochemistry and tectonic setting of the lower Proterozoic supracrustal rocks of the Pinal Schist, southeastern Arizona: Geol. Soc. America Bull., v. 97, p. 1512–1520.

Cornwall, H. R., and Krieger, M. H., 1978, Geologic map of the El Capitan Mountain quadrangle, Gila and Pinal Counties, Arizona: U.S. Geol. Survey Map GQ-1442, Scale, 1:24,000.

DePaolo, D. J., 1981, Neodymium isotopes in the Colorado Front Range and crust-mantle evolution in the Proterozoic: Nature, v. 271, p. 193–196.

Drewes, H., 1981, Tectonics of southeastern Arizona: U.S. Geol. Survey Prof. Paper 1144.

Dubendorfer, E. M., and Houston, R. S., 1987, Proterozoic accretionary tectonics at the southern margin of the Archean Wyoming craton: Geol. Soc. America Bull., v. 98, p. 554–568.

Erickson, R. C., 1968, Geology and geochronology of the Dos Cabezas Mountains, Cochise County, Arizona: Arizona Geol. Soc. Guidebook 3, p. 193–198.

Gapais, D.; Bale, P.; Choukroune, P.; Cobbold, P. R.; Mahjoub, Y.; and Marquer, D., 1987, Bulk kinematics from shear zone patterns: Some field examples: Jour. Struct. Geol., v. 9, p. 635–646.

Garbutt, J. M., and Teyssier, C., 1991, Prism ⟨c⟩ slip in the quartzites of the Oakhurst mylonite belt, California: Jour. Struct. Geol., v. 13, p. 657–666.

Garcia Celma, A., 1982, Domainal and fabric heterogeneities in the Cap de Creus mylonites: Jour. Struct. Geol., v. 4, p. 443–455.

Hirth, G., and Tullis, J., 1992, Dislocation creep regimes in quartz aggregates: Jour. Struct. Geol., v. 14, p. 145–159.

Jessell, M. W., and Lister, G. S., 1990, A simulation of the temperature dependence of quartz fabrics, *in* Knipe, R. J., and Rutter, E. H., eds., Deformation mechanisms, rheology, and tectonics: Geol. Soc. London Spec. Pub. 54, p. 353–362.

Karlstrom, K. E.; Bowring, S. A.; and Conway, C. M., 1987, Tectonic significance of an early Proterozoic two-province boundary in central Arizona: Geol. Soc. America Bull., v. 99, p. 529–538.

———, and ———, 1988, Early Proterozoic assembly of tectonostratigraphic terranes in southwestern North America: Jour. Geology, v. 96, p. 561–576.

Keep, M., and Hansen, V. L., 1991, Structural and kinematic analysis of the Pinal Schist in the Mineral Mountain quadrangle, Pinal County, Arizona: Geol. Soc. America Abs. with Prog., v. 23, p. 37.

———, and ———, 1993, Deformation styles in the Proterozoic Pinal Schist, Pinal Mountains, Arizona: Geol. Soc. America Abs. with Prog., v. 25, p. 17.

Krohe, A., 1990, Local variations in quartz [*c*]-axis orientations in non-coaxial regimes and their significance for the mechanisms of S-C fabrics: Jour. Struct. Geol., v. 12, p. 995–1004.

Law, R. D., 1990, Crystallographic fabrics: a selective review of their applications to research in structural geology, *in* Knipe, R. J., and Rutter, E. H., eds., Deformation mechanisms, rheology, and tectonics: Geol. Soc. London Spec. Pub. 54, p. 335–352.

———; Miller, E. L.; Little, T. A.; and Lee, J., 1994, Extensional origin of ductile fabrics in the Schist Belt, Central Brooks Range, Alaska—II. Microstructural and petrofabric evidence: Jour. Struct. Geol., in press.

Lister, G. S., 1977, Discussion: Cross girdle *c*-axis fabrics in quartzites plastically deformed by plane strain and progressive simple shear: Tectonophysics, v. 39, p. 51–54.

———, and Dornsiepen, U. F., 1982, Fabric transitions in the Saxony granulite terrain: Jour. Struct. Geol., v. 4, p. 81–92.

———, and Hobbs, B. E., 1980, The simulation of fabric development during plastic deformation history and its application to quartzite: the influence of deformation history: Jour. Struct. Geol., v. 2, p. 355–370.

———, and Price, G. P., 1978, Fabric development in a quartz-feldspar mylonite: Tectonophysics, v. 49, p. 37–78.

———, and Snoke, A. W., 1984, S-C mylonites: Jour. Struct. Geol., v. 6, p. 617–638.

———, and Williams, P. F., 1979, Fabric development in

shear zones: theoretical controls and observed phenomena: Jour. Struct. Geol., v. 1, p. 282–298.

———, and ———, 1983, The partitioning of deformation in flowing rock masses: Tectonophysics, v. 92, p. 1–33.

Livingston, D. E., 1969, Geochronology of older Precambrian rocks of Gila County, Arizona: Unpub. Ph.D. dissertation, University of Arizona, Tucson.

Miller, D. M., and Christie, J. M., 1981, Comparison of quartz microfabric with strain in recrystallized quartzite: Jour. Struct. Geol., v. 3, p. 129–141.

Nelson, B. K., and DePaolo, D. J., 1984, 1,700 Myr greenstone volcanic successions in southwestern North America and isotope evolution of Proterozoic mantle: Nature, v. 312, p. 143–146.

———, and ———, 1985, Rapid production of continental crust 1.7 to 1.9 b.y. ago: Nd isotopic evidence from the basement of the North American mid-continent: Geol. Soc. America Bull., v. 96, p. 746–754.

Passchier, C. W., 1983, The reliability of asymmetric *c*-axis fabrics of quartz to determine sense of vorticity: Tectonophysics, v. 99, p. T9–T18.

———, and Simpson, C., 1986, Porphyroclast systems as kinematic indicators: Jour. Struct. Geol., v. 8, p. 831–844.

Peterson, N. P., 1962, Geology and ore deposits of the Globe-Miami district, Arizona: U.S. Geol. Survey Prof. Paper 342, 151 p.

Price, G. D., 1985, Preferred orientations in quartzites, *in* Wenk, H.-R. ed., Preferred Orientation in Deformed Metals and Rocks: An Introduction to Modern Texture Analysis: Orlando, Academic Press, p. 385–406.

Ralser, S.; Hobbs, B. E.; and Ord, A., 1991, Experimental deformation of a quartz mylonite: Jour. Struct. Geology, v. 13, p. 837–850.

Ransome, F. L., 1903, Geology of the Globe copper district, Arizona: U.S. Geol. Survey Prof. Paper 12, 168 p.

———, 1904, Description of the Globe quadrangle, Arizona: U.S. Geol. Survey Atlas Folio, v. 111, p. 17.

———, 1919, The copper deposits of Ray and Miami, Arizona: U.S. Geol. Survey Prof. Paper 115, 192 p.

Sander, B., 1970, An Introduction to the Study of Fabrics of Geologic Bodies (1st Eng. ed.): Oxford, Pergamon, 641 p.

Schmid, S. M., and Casey, M., 1986, Complete fabric analysis of some commonly observed quartz *c*-axes patterns, *in* Hobbs, B. E., and Heard, M. C., eds., Mineral and rock deformation: Laboratory studies—the Paterson Volume: Am. Geophys. Union Mon. 36, p. 263–286.

Sease, G. D., 1993, Structural and kinematic analysis of Middle Proterozoic tectonites, Dos Cabezas Mountains, Arizona: Unpub. M.Sc. thesis, Southern Methodist University, Dallas.

———, and Hansen, V. L., 1990, Structural and kinematic analysis of the Middle Proterozoic Dos Cabezas shear zone, Dos Cabezas Mountains, southeast Arizona: Geol. Soc. America Abs. with Prog., v. 22, p. 82.

Simpson, C., 1985, Deformation of granitic rocks across the brittle-ductile transition: Jour. Struct. Geol., v. 7, p. 503–511.

———, 1986, Determination of movement sense in mylonites: Jour. Geol. Education, v. 34, p. 246–261.

———, and Schmid, S. M., 1983, An evaluation of criteria to deduce the sense of movement in sheared rocks: Geol. Soc. America Bull., v. 94, p. 1281–1288.

Stacey, J. S., and Hedlund, D. C., 1983, Lead isotope compositions of diverse igneous rocks and ore deposits from southwestern New Mexico and their implications for Early Proterozoic crustal evolution in the western United States: Geol. Soc. America Bull., v. 94, p. 43–57.

Starkey, J., 1987, Analysis of orientation diagrams derived from a simulated quartz fabric: Can. Jour. Earth Sci., v. 24, p. 565–571.

———, and Cutforth, C., 1978, A demonstration of the interdependence of the degree of quartz preferred orientation and the quartz content in deformed rocks: Can. Jour. Earth Sci., v. 15, p. 841–847.

Swift, P. N., 1987, Early Proterozoic turbidite deposition and melange deformation, southeastern Arizona: Unpub. Ph.D. dissertation, University of Arizona, Tucson.

Theodore, T. G.; Keith, W. J.; Till, A. B.; and Peterson, J. A., 1978, Preliminary geologic map of the Mineral Mountain 7 1/2 quadrangle, Arizona: U.S. Geol. Survey Open File Rept. 78-468, scale, 1:24,000.

Tullis, J., 1977, Preferred orientation of quartz produced by slip during plane strain: Tectonophysics, v. 39, p. 87–102.

———; Christie, J. M.; and Griggs, D. T., 1973, Microstructures and preferred orientations of experimentally deformed quartz: Geol. Soc. America Bull., v. 84, p. 297–314.

Van-Schmus, W. R., and Bickford, M. E., 1981, Proterozoic chronology and evolution of the midcontinent region, North America, *in* Kröner, A., ed., Precambrian Plate Tectonics: New York, Elsevier, p. 261–296.

Williams, M. L., 1991, Overview of Proterozoic metamorphism in Arizona, *in* Karlstrom, K. E., ed., Proterozoic geology and ore deposits of Arizona: Arizona Geol. Soc. Digest, v. 19, p. 11–26.

Wilson, E. D., 1939, Precambrian Mazatzal revolution in central Arizona: Geol. Soc. America Bull., v. 50, p. 1113–1164.

———; Moore, R. T.; and Cooper, J. R., 1969, Geologic map of Arizona: Arizona Bureau of Mines, scale, 1:500,000.

Wooden, J. L., 1991, Early Proterozoic isotopic provinces in the southwestern U.S.: Geol. Soc. America Abs. with Prog., v. 23, p. 107.

———, and DeWitt, E., 1991, Pb isotopic evidence for the boundary between the Early Proterozoic Mojave and Central Arizona crustal provinces in western Arizona, *in* Karlstrom, K. E., eds., Proterozoic geology and ore deposits of Arizona: Arizona Geol. Soc. Digest, v. 19, p. 27–50.